Progress In Electromagnetics Research M, Vol. 17, 253–265, 2011

A FUNDAMENTAL LIMIT ON SUBWAVELENGTH GUIDED WAVES

A. Arbabi

Department of Electrical and Computer Engineering
University of Waterloo
200 University Avenue West, Waterloo, Ontario N2L 3G1, Canada

E. Arbabi

School of Electrical and Computer Engineering
University of Tehran, North Kargar Ave., Tehran, Iran

S. Safavi-Naeini

Department of Electrical and Computer Engineering,
University of Waterloo
200 University Avenue West, Waterloo, Ontario N2L 3G1, Canada

Abstract—A fundamental relation between the cross sectional confinement of an arbitrary mode of a general waveguide and its propagation length is found. It is shown that due to material loss of the waveguide, the propagation length shrinks as the confinement of the mode increases. Normalized second central moment of magnetic energy density in the cross section plane of the waveguide is used as a measure of mode size and it is found that for a given mode size, there is a limit for the waveguide propagation length. This limit depends solely on permittivity of the waveguide material and its surrounding medium. As an application, this result provides a lower bound for propagation loss in subwavelength optical confinement in plasmonic waveguides which are of special interest for their nano-meter mode dimensions.

Received 29 January 2011, Accepted 28 March 2011, Scheduled 30 March 2011
Corresponding author: Amir Arbabi (aarbabi@maxwell.uwaterloo.ca).

1. INTRODUCTION

In recent years, with the advent of the emerging field of surface plasmon photonics or so called "Plasmonics" [1, 2], subwavelength waveguides at optical frequencies have attracted much attention. Different types of waveguides have been proposed and investigated for their ability to guide optical waves with subwavelength cross sectional mode dimensions [3–11]. Based on these waveguides, several passive and active devices and elements such as bends, interferometers, filters, resonators, and lasers have been introduced [12–15]. Although waveguides with subwavelength mode dimensions such as coaxial and microstrip lines have been used at microwave and lower frequencies without a significant loss, at higher frequencies metal dissipative loss has been an obstacle for plasmonic waveguides to find practical application. In some of the studies in this area, it has been noted that there is a trade-off between the confinement of a waveguide mode and its attenuation constant [8, 16]. In this paper, it is shown that regardless of the waveguide shape, for a given mode size, a fundamental lower bound on the attenuation constant exists.

The existence of such a limit is a generalization of the diffraction limit which sets a lower bound on confinement of free propagating waves. Therefore, the approach which is used in this paper is similar to the one used for deriving the diffraction limit. The fields are considered in spectral domain and the waveguide is replaced with an equivalent free current distribution. This is this current distribution which allows for confinement beyond the diffraction limit, and because it is supported by the lossy waveguide material, it causes the propagation loss.

2. PROBLEM FORMULATION

A general waveguide made of a non-magnetic material with permittivity of $\epsilon_r = \epsilon_r' - j\epsilon_r''$ surrounded by a lossless material with permittivity of ϵ_s is considered (Fig. 1). The surrounding material may fill the entire space around the waveguide or only the space near the waveguide where the fields have significant values. It is assumed that the waveguide structure has no variation in the direction of its axis and the coordinate system is chosen in a way that its z axis is aligned with the waveguide axis. The time dependency of $\mathrm{e}^{j\omega t}$ and z variation of $\mathrm{e}^{-j\gamma z}$, $\gamma = \beta - j\alpha$, are assumed where β and α are phase and attenuation constants, respectively. The electric and magnetic fields of a waveguide mode satisfy the Maxwell's equations in the entire space

$$\nabla \times \mathbf{E} = -j\omega\mu_0\mathbf{H} \tag{1a}$$

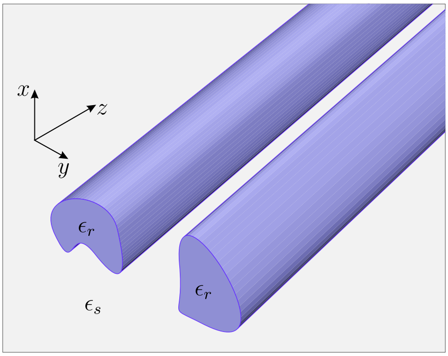

Figure 1. A general waveguide structure composed of lossy dielectrics with relative permittivity of ϵ_r surrounded by lossless material with permittivity of ϵ_s. z axis of the coordinate system is parallel to the waveguide axis.

$$\nabla \times \mathbf{H} = j\omega\epsilon_0\epsilon_s\mathbf{E} + \mathbf{J} \tag{1b}$$

$$\nabla \cdot \mathbf{E} = \frac{j}{\omega\epsilon_0\epsilon_s}\nabla \cdot \mathbf{J} \tag{1c}$$

$$\nabla \cdot \mathbf{H} = 0 \tag{1d}$$

with $\mathbf{J}$ representing the equivalent current density defined as

$$\mathbf{J} = j\omega\epsilon_0(\epsilon - \epsilon_s)\mathbf{E}. \tag{2}$$

ϵ is position dependent relative permittivity. Therefore, the waveguide is replaced by an equivalent volume current density which is nonzero only where the waveguide is placed and zero elsewhere. From the Maxwell's equations, second order equations for electric and magnetic fields can be derived as

$$\nabla^2\mathbf{E} + k^2\mathbf{E} = \frac{j}{\omega\epsilon_0\epsilon_s}\left(k^2\mathbf{J} + \nabla(\nabla \cdot \mathbf{J})\right) \tag{3}$$

$$\nabla^2\mathbf{H} + k^2\mathbf{H} = -\nabla \times \mathbf{J}, \tag{4}$$

where $k = \omega\sqrt{\epsilon_s\epsilon_0\mu_0}$ is the wave number in the surrounding medium. Equation (1a) can be written as

$$\nabla \times \left(\mathbf{E}\mathrm{e}^{j\gamma z}\mathrm{e}^{-j\gamma z}\right) = -j\omega\mu_0\mathbf{H}. \tag{5}$$

Using the identity for curl of product of a scalar and a vector, left hand side of (5) can be expended as

$$\nabla \times \left(\mathbf{E}\mathrm{e}^{j\gamma z}\right)\mathrm{e}^{-j\gamma z} - j\gamma\left(\hat{z} \times \mathbf{E}\right) = -j\omega\mu_0\mathbf{H}. \tag{6}$$

Scalar multiplication of both sides of (6) by $\mathbf{H}^*$ and integrating over waveguide cross section (x-y plane) gives

$$S=\frac{1}{2}\int\mathbf{E}\times\mathbf{H}^*\cdot\hat{z}\mathrm{d}a=\frac{\omega\mu_0}{2\gamma}\int|\mathbf{H}|^2\mathrm{d}a+\frac{\mathrm{e}^{-j\gamma z}}{j2\gamma}\int\nabla\times\left(\mathbf{E}\mathrm{e}^{j\gamma z}\right)\cdot\mathbf{H}^*\mathrm{d}a. \quad (7)$$

Here $\mathrm{d}a = \mathrm{d}x\mathrm{d}y$ is the differential of the cross sectional area and the integrals in (7) and all other integrals in this paper are taken over the entire cross sectional plane. S is complex power passing through the waveguide cross section. It should be noted that for a mode with propagation constant of γ, $\mathbf{E}\mathrm{e}^{j\gamma z}$ has no z dependence. It is useful to define

$$\mathbf{F} \triangleq \nabla \times \left(\mathbf{E}\mathrm{e}^{j\gamma z}\right). \quad (8)$$

The material loss of the waveguide per unit length can be found using (2)

$$P_l = \frac{1}{2}\mathrm{Re}\left\{\int \mathbf{E}\cdot\mathbf{J}^*\mathrm{d}a\right\} = \frac{\epsilon_r''}{2\omega\epsilon_0|\epsilon_r-\epsilon_s|^2}\int|\mathbf{J}|^2\mathrm{d}a, \quad (9)$$

and using the Poynting's theorem for an infinitesimal slice of waveguide along its axis, the attenuation constant can be shown to be given by

$$\alpha = \frac{P_l}{2\mathrm{Re}\{S\}}. \quad (10)$$

Attenuation constant shows the waveguide propagation loss. As a criterion for the mode confinement, the normalized second central moment of the magnetic energy density in the waveguide cross section can be used. For a normalized mode with $\int|\mathbf{H}|^2\mathrm{d}a = 1$, this central moment is defined as

$$\sigma_{\mathbf{H}}^2 = \int r^2|\mathbf{H}|^2\mathrm{d}a - \left(\int x|\mathbf{H}|^2\mathrm{d}a\right)^2 - \left(\int y|\mathbf{H}|^2\mathrm{d}a\right)^2. \quad (11)$$

It will be shown that for an arbitrary waveguide mode with a given value for the second central moment, a lower limit for the attenuation constant of the mode exists. To this end, the fields are considered in the spectral domain.

3. SPECTRAL DOMAIN EXPRESSIONS FOR WAVEGUIDE LOSS AND MODE SIZE

The spectral domain representation of a vectorial quantity such as $\mathbf{U}$ is defined as the Fourier transform of that vector in cross sectional plane of the waveguide

$$\tilde{\mathbf{U}}(k_x,k_y,z) = \int \mathbf{U}(x,y,z)\mathrm{e}^{-j(k_x x+k_y y)}\mathrm{d}a, \quad (12)$$

and the inverse transform is given by

$$\mathbf{U}(x,y,z)=\frac{1}{4\pi^2}\int\tilde{\mathbf{U}}(k_x,k_y,z)\mathrm{e}^{j(k_xx+k_yy)}\mathrm{d}s. \tag{13}$$

In (13), $\mathrm{d}s=\mathrm{d}k_x\mathrm{d}k_y$ represents the differential of area in the spectral domain and the integrals is over the entire k_x-k_y plane. In the spectral domain, (3) and (4) can be written as

$$\tilde{\mathbf{E}}=\begin{bmatrix}\tilde{E}_x\\ \tilde{E}_y\\ \tilde{E}_z\end{bmatrix}=\frac{1}{j\omega\epsilon_0\epsilon_s(k_r^2+\gamma^2-k^2)}[\mathcal{M}]\tilde{\mathbf{J}} \tag{14}$$

$$\tilde{\mathbf{H}}=\begin{bmatrix}\tilde{H}_x\\ \tilde{H}_y\\ \tilde{H}_z\end{bmatrix}=\frac{1}{(k_r^2+\gamma^2-k^2)}[\mathcal{B}]\tilde{\mathbf{J}} \tag{15}$$

where $k_r^2=k_x^2+k_y^2$, and $[\mathcal{M}]$ and $[\mathcal{B}]$ matrices are given by

$$[\mathcal{M}]=\begin{pmatrix}k^2-k_x^2 & -k_xk_y & -k_x\gamma\\ -k_xk_y & k^2-k_y^2 & -k_y\gamma\\ -k_x\gamma & -k_y\gamma & k^2-\gamma^2\end{pmatrix} \tag{16}$$

$$[\mathcal{B}]=\begin{pmatrix}0 & j\gamma & -jk_y\\ -j\gamma & 0 & jk_x\\ jk_y & -jk_x & 0\end{pmatrix}. \tag{17}$$

Using (8) and (14) the spectral representation of $\mathbf{F}$ can be found as:

$$\tilde{\mathbf{F}}=\frac{\mathrm{e}^{j\gamma z}}{j\omega\epsilon_0\epsilon_s(k_r^2+\gamma^2-k^2)}[\mathcal{N}]\tilde{\mathbf{J}} \tag{18}$$

where $[\mathcal{N}]$ is defined as

$$[\mathcal{N}]=j\begin{pmatrix}k_xk_y\gamma & k_y^2\gamma & -k_y\left(k^2-\gamma^2\right)\\ -k_x^2\gamma & -k_xk_y\gamma & k_x\left(k^2-\gamma^2\right)\\ k^2k_y & -k^2k_x & 0\end{pmatrix}. \tag{19}$$

Now, by use of the Parseval's theorem,

$$\int\mathbf{V}^*\cdot\mathbf{U}\mathrm{d}a=\frac{1}{4\pi^2}\int\tilde{\mathbf{V}}^\dagger\tilde{\mathbf{U}}\mathrm{d}s, \tag{20}$$

S and P_l can be expressed in terms of spectral domain vectors. Multiplying each side of (15) by their Hermitian transpose gives

$$|\tilde{\mathbf{H}}|^2=\tilde{\mathbf{H}}^\dagger\tilde{\mathbf{H}}=\frac{1}{|k_r^2+\gamma^2-k^2|^2}\tilde{\mathbf{J}}^\dagger[\mathcal{B}]^\dagger[\mathcal{B}]\tilde{\mathbf{J}}. \tag{21}$$

By defining

$$[\mathcal{A}]\triangleq[\mathcal{B}]^\dagger[\mathcal{B}] \tag{22}$$

and using (20), it can be found that

$$\int |\mathbf{H}|^2 \mathrm{d}a = \frac{1}{4\pi^2} \int \frac{1}{|k_r^2 + \gamma^2 - k^2|^2} \tilde{\mathbf{J}}^\dagger [\mathcal{A}] \tilde{\mathbf{J}} \mathrm{d}s. \tag{23}$$

From (15), (18), and (20) give

$$\int \mathbf{H}^* \cdot \mathbf{F} \mathrm{d}a = \frac{1}{4\pi^2} \int \tilde{\mathbf{H}}^\dagger \tilde{\mathbf{F}} \mathrm{d}s = \frac{-j\mathrm{e}^{j\gamma z}}{4\pi^2 \omega \epsilon_0 \epsilon_s} \int \frac{1}{|k_r^2 + \gamma^2 - k^2|^2} \tilde{\mathbf{J}}^\dagger [\mathcal{B}]^\dagger [\mathcal{N}] \tilde{\mathbf{J}} \mathrm{d}s. \tag{24}$$

Substituting two left hand side integrals in (23) and (24) into (7) leads to

$$S = \frac{1}{8\pi^2 \omega \epsilon_0 \epsilon_s} \int \frac{1}{|k_r^2 + \gamma^2 - k^2|^2} \tilde{\mathbf{J}}^\dagger [\mathcal{Z}] \tilde{\mathbf{J}} \mathrm{d}s, \tag{25}$$

where $[\mathcal{Z}]$ is defined as

$$[\mathcal{Z}] \triangleq \frac{1}{\gamma} \left(k^2 [\mathcal{A}] - [\mathcal{B}]^\dagger [\mathcal{N}] \right). \tag{26}$$

Material loss of the waveguide can also be expressed in terms of spectral domain volume current density. From (9) and (20), P_l can be expressed in terms of spectral representation of the current density

$$P_l = \frac{\epsilon_r''}{8\pi^2 \omega \epsilon_0 |\epsilon_r - \epsilon_s|^2} \int \left| \tilde{\mathbf{J}} \right|^2 \mathrm{d}s. \tag{27}$$

Finally, the attenuation constant of the waveguide can be found by substituting S and P_l from (25) and (9) into (10)

$$\alpha = \frac{\epsilon_s \epsilon_r''}{2 \left| \epsilon_r - \epsilon_s \right|^2} \frac{\int \left| \tilde{\mathbf{J}} \right|^2 \mathrm{d}s}{\int \frac{1}{|k_r^2 + \gamma^2 - k^2|^2} \mathrm{Re} \left\{ \tilde{\mathbf{J}}^\dagger [\mathcal{Z}] \tilde{\mathbf{J}} \right\} \mathrm{d}s}. \tag{28}$$

As a criterion for the mode size in the spectral domain, the normalized second central moment of the spectral domain magnetic field modulus squared can be used. This moment is later related to the magnetic density moment defined in (11). For a normalized mode such that

$$\int \left| \tilde{\mathbf{H}} \right|^2 \mathrm{d}s = 1, \tag{29}$$

the second central moment of the magnetic field modulus squared in spectral domain is defined similar to (11) as

$$\sigma_{\tilde{\mathbf{H}}}^2 = \int k_r^2 \left| \tilde{\mathbf{H}} \right|^2 \mathrm{d}s - \left(\int k_x \left| \tilde{\mathbf{H}} \right|^2 \mathrm{d}s \right)^2 - \left(\int k_y \left| \tilde{\mathbf{H}} \right|^2 \mathrm{d}s \right)^2. \tag{30}$$

4. UPPER LIMIT ON THE WAVEGUIDE PROPAGATION LENGTH

In the followings, for a given value of $\sigma^2_{\tilde{\mathbf{H}}}$ a lower bound for the attenuation constant will be found and later $\sigma^2_{\tilde{\mathbf{H}}}$ will be related to the $\sigma^2_{\mathbf{H}}$. For this goal, eigenvectors and eigenvalues of $[\mathcal{A}]$ can be used to choose $\tilde{\mathbf{J}}$ in a way to minimize the attenuation constant. Eigenvalues and normalized eigenvectors of $[\mathcal{A}]$ can be found to be:

$$\hat{V}_{\mathcal{A}_1} = \frac{1}{k_r}\begin{bmatrix} k_y \\ -k_x \\ 0 \end{bmatrix}, \qquad \lambda_{\mathcal{A}_1} = k_r^2 + |\gamma|^2 \tag{31a}$$

$$\hat{V}_{\mathcal{A}_2} = \frac{|\gamma|}{k_r\sqrt{k_r^2 + |\gamma|^2}}\begin{bmatrix} k_x \\ k_y \\ -\frac{k_r^2}{\gamma^*} \end{bmatrix}, \qquad \lambda_{\mathcal{A}_2} = k_r^2 + |\gamma|^2 \tag{31b}$$

$$\hat{V}_{\mathcal{A}_3} = \frac{1}{\sqrt{k_r^2 + |\gamma|^2}}\begin{bmatrix} k_x \\ k_y \\ \gamma \end{bmatrix}, \qquad \lambda_{\mathcal{A}_3} = 0. \tag{31c}$$

$[\mathcal{A}]$ is hermitian and its normalized eigenvectors are three independent, mutually orthogonal vectors and constitute a orthonormal basis. Therefore, the volume current density in the spectral domain can be expanded in terms of them

$$\tilde{\mathbf{J}} = c_1\hat{V}_{\mathcal{A}_1} + c_2\hat{V}_{\mathcal{A}_2} + c_3\hat{V}_{\mathcal{A}_3}, \tag{32}$$

where coefficients c_i are functions of k_x and k_y. Using (28), the attenuation constant can be expressed in terms of theses coefficients. More specifically, $|\tilde{\mathbf{J}}|^2$ in the numerator of the right hand side of this equation can be written as

$$\left|\tilde{\mathbf{J}}\right|^2 = |c_1|^2 + |c_2|^2 + |c_3|^2, \tag{33}$$

and for expressing $\mathrm{Re}\{\tilde{\mathbf{J}}^\dagger[\mathcal{Z}]\tilde{\mathbf{J}}\}$ in the denominator, the following relations can be used:

$$[\mathcal{Z}]\hat{V}_{\mathcal{A}_1} = \left(k^2\beta + j\alpha k^2\right)\hat{V}_{\mathcal{A}_1} \tag{34a}$$

$$[\mathcal{Z}]\hat{V}_{\mathcal{A}_2} = \left(k^2\beta + j\alpha\left(k^2 - 2k_r^2\right)\right)\hat{V}_{\mathcal{A}_2} \tag{34b}$$

$$[\mathcal{Z}]\hat{V}_{\mathcal{A}_3} = \frac{\gamma^*}{|\gamma|}k_r\left(k^2 - k_r^2 - \gamma^2\right)\hat{V}_{\mathcal{A}_2}. \tag{34c}$$

Equations (34) can be verified by direct calculation of $[\mathcal{Z}]$ from (26) and eigenvectors of $[\mathcal{A}]$ given in (31). Using these relations and (32),

$\mathrm{Re}\{\tilde{\mathbf{J}}^\dagger[\mathcal{Z}]\tilde{\mathbf{J}}\}$ can be found as

$$\mathrm{Re}\left\{\tilde{\mathbf{J}}^\dagger[\mathcal{Z}]\tilde{\mathbf{J}}\right\}=k^2\beta\left(|c_1|^2+|c_2|^2\right)+\mathrm{Re}\left\{\frac{\gamma^*}{|\gamma|}k_r\left(k^2-k_r^2-\gamma^2\right)c_2^*c_3\right\}. \quad (35)$$

plugging $|\tilde{\mathbf{J}}|^2$ and $\mathrm{Re}\{\tilde{\mathbf{J}}^\dagger[\mathcal{Z}]\tilde{\mathbf{J}}\}$ from (33) and (35) into (28), results in:

$$\alpha=\frac{\epsilon_s\epsilon_r''}{2|\epsilon_r-\epsilon_s|^2}\frac{\int\left(|c_1|^2+|c_2|^2\right)\mathrm{d}s+\int|c_3|^2\mathrm{d}s}{k^2\beta\int\frac{|c_1|^2+|c_2|^2}{|k_r^2+\gamma^2-k^2|^2}\mathrm{d}s+\int\frac{\mathrm{Re}\left\{\frac{\gamma^*}{|\gamma|}k_r(k^2-k_r^2-\gamma^2)c_2^*c_3\right\}}{|k_r^2+\gamma^2-k^2|^2}\mathrm{d}s}. \quad (36)$$

The square modulus of the spectral domain magnetic field can also be expressed in terms of the c_i coefficients. Equations (21) and (32) lead to

$$\left|\tilde{\mathbf{H}}\right|^2=\frac{k_r^2+|\gamma|^2}{|k_r^2+\gamma^2-k^2|^2}\left(|c_1|^2+|c_2|^2\right). \quad (37)$$

It can be observed from (37) that $|\tilde{\mathbf{H}}|^2$ and therefore $\sigma_{\tilde{\mathbf{H}}}^2$ does not depend on c_3. Thus, c_3 can be chosen freely to minimize the attenuation constant. In the (36), for a given value of $\int|c_3|^2\mathrm{d}s$ in the numerator, based on the Cauchy-Schwarz inequality, the integral involving c_3 in the denominator achieves its maximum when

$$c_3=a\frac{k_r\gamma}{|\gamma|(k^2-\gamma^2-k_r^2)}c_2, \quad (38)$$

where a is a positive real number. Plugging in c_3 from (38) into (36) and expressing $|c_1|^2+|c_2|^2$ using (37) gives

$$\alpha\geq\frac{\epsilon_s\epsilon_r''}{2\left|\epsilon_r-\epsilon_s\right|^2}\frac{\int\frac{\left|k_r^2+\gamma^2-k^2\right|^2}{k_r^2+|\gamma|^2}\left|\tilde{\mathbf{H}}\right|^2\mathrm{d}s+a^2\int\frac{k_r^2|c_2|^2}{|k_r^2+\gamma^2-k^2|^2}\mathrm{d}s}{k^2\beta\int\frac{1}{k_r^2+|\gamma|^2}\left|\tilde{\mathbf{H}}\right|^2\mathrm{d}s+a\int\frac{k_r^2|c_2|^2}{|k_r^2+\gamma^2-k^2|^2}\mathrm{d}s}. \quad (39)$$

Let us define:

$$b\triangleq\int\frac{\left|k_r^2+\gamma^2-k^2\right|^2}{k_r^2+|\gamma|^2}\left|\tilde{\mathbf{H}}\right|^2\mathrm{d}s \quad (40a)$$

$$u\triangleq\int\frac{k_r^2|c_2|^2}{|k_r^2+\gamma^2-k^2|^2}\mathrm{d}s \quad (40b)$$

$$d\triangleq k^2\beta\int\frac{1}{k_r^2+|\gamma|^2}\left|\tilde{\mathbf{H}}\right|^2\mathrm{d}s \quad (40c)$$

Using these definitions, (39) can be rewritten as

$$\alpha\geq\frac{\epsilon_s\epsilon_r''}{2|\epsilon_r-\epsilon_s|^2}\frac{b+ua^2}{d+ua}. \quad (41)$$

Right hand side of (41) is larger than its minimum value for different values of a and this results in

$$\alpha \geq \frac{\epsilon_s \epsilon_r''}{2|\epsilon_r - \epsilon_s|^2} \frac{b + ua^2}{d + ua} \geq \frac{\epsilon_s \epsilon_r''}{|\epsilon_r - \epsilon_s|^2} \frac{1}{u} \left(\sqrt{bu + d^2} - d \right). \tag{42}$$

It can be verified that $\frac{1}{u}\left(\sqrt{bu + d^2} - d\right)$ is a decreasing function of u and its substitution by q defined as

$$q \triangleq \int \frac{k_r^2 \left(|c_1|^2 + |c_2|^2\right)}{|k_r^2 + \gamma^2 - k^2|^2} \mathrm{d}s = \int \frac{k_r^2}{k_r^2 + |\gamma|^2} \left|\tilde{\mathbf{H}}\right|^2 \mathrm{d}s \geq u, \tag{43}$$

results in a lower limit for $\frac{1}{u}(\sqrt{bu + d^2} - d)$ and therefore for α, that is

$$\alpha \geq \frac{\epsilon_s \epsilon_r''}{|\epsilon_r - \epsilon_s|^2} \frac{1}{q} \left(\sqrt{bq + d^2} - d \right). \tag{44}$$

In many cases of interest $\frac{\alpha}{k} \ll 1$ and α^2 can be neglected. Neglecting terms involving α^2 in b, q, and d, defining p as $p \triangleq \int k_r^2 |\tilde{\mathbf{H}}|^2 \mathrm{d}s + \beta^2 - 2k^2$, and using (29), it can be found that

$$b = p + \frac{k^4}{\beta^2}(1 - q), \tag{45a}$$

$$d = \frac{k^2}{\beta}(1 - q). \tag{45b}$$

Plugging in b and d from (45) into (44) gives

$$\alpha \geq \frac{\epsilon_s \epsilon_r''}{|\epsilon_r - \epsilon_s|^2} \frac{1}{q} \left(\sqrt{pq + \frac{k^4}{\beta^2}(1 - q)} - \frac{k^2}{\beta}(1 - q) \right), \tag{46}$$

and it is easy to verify that the right hand side of the inequality (46) is a decreasing function of q. It can also be observed from the definition of q that $0 < q \leq \int |\tilde{\mathbf{H}}|^2 \mathrm{d}s = 1$, therefore putting $q = 1$ gives a lower bound for that expression, that is

$$\alpha > \frac{\epsilon_s \epsilon_r''}{|\epsilon_r - \epsilon_s|^2} \sqrt{p} = \frac{\epsilon_s \epsilon_r''}{|\epsilon_r - \epsilon_s|^2} \sqrt{\int k_r^2 \left|\tilde{\mathbf{H}}\right|^2 \mathrm{d}s + \beta^2 - 2k^2}, \tag{47}$$

and from (30) it is obvious that $\int k_r^2 |\tilde{\mathbf{H}}|^2 \mathrm{d}s \geq \sigma_{\tilde{\mathbf{H}}}^2$, therefore

$$\alpha > \frac{\epsilon_s \epsilon_r''}{|\epsilon_r - \epsilon_s|^2} \sqrt{\sigma_{\tilde{\mathbf{H}}}^2 + \beta^2 - 2k^2}. \tag{48}$$

The uncertainty relation for the two dimensional Fourier transform requires

$$\sigma_{\mathbf{H}}^2 \sigma_{\tilde{\mathbf{H}}}^2 \geq 1 \tag{49}$$

combining (48) and (49) and noticing that for guided modes $\beta > k$ (48) can be further simplified as

$$\alpha > \frac{\epsilon_s \epsilon_r''}{|\epsilon_r - \epsilon_s|^2} \sqrt{\frac{1}{\sigma_{\mathbf{H}}^2} - k^2}. \tag{50}$$

Expressing attenuation constant in terms of propagation length ($L = \frac{1}{\alpha}$), (50) becomes

$$\frac{L}{\lambda} < \frac{|\epsilon_r - \epsilon_s|^2}{\epsilon_s \epsilon_r''} \frac{1}{\sqrt{\left(\frac{\lambda}{\sigma_{\mathbf{H}}}\right)^2 - 4\pi^2}}. \tag{51}$$

5. DISCUSSION OF THE RESULT AND NUMERICAL EXAMPLES

The inequality (51) shows that for a given waveguide mode size and core material, there is a upper limit on the propagation length. As it was mentioned earlier, the limit is the result of the dissipative loss of the waveguide core material. For achieving sub-diffraction limit confinement of waves, a nonzero equivalent current density should exist. As it was shown, higher confinement requires a larger equivalent current density. Because the equivalent current density is supported by the waveguide core the higher equivalent current density means larger dissipative loss and therefore shorter propagation length.

As it can be seen from (51), the material properties are only present as a multiplicative factor. In particular, for waveguides with air as surrounding material we can define a material loss merit factor as

$$M \triangleq \frac{|\epsilon_r - 1|^2}{\epsilon_r''} \tag{52}$$

This merit factor can be used for determining preferred waveguide materials.

It is also interesting to compare the propagation lengths of some simple plasmonic waveguides with the upper limit given in (51). According to (51), a waveguide made of gold and surrounded by vacuum with subwavelength mode size of $\sigma_{\mathbf{H}} = 100\,\text{nm}$ at $\lambda = 1.55\,\mu\text{m}$ ($\epsilon_{r_{Au}} \simeq -95.9 - j11$ [17]) has a propagation length shorter than 61.02λ. Fig. 2 shows the schematics and magnetic energy distributions of few waveguide modes at $\lambda = 1.55\,\mu\text{m}$. The waveguides are assumed to be made of gold and surrounded by vacuum. The fields distributions and propagation constants of these modes are found using the Finite Element Method (FEM). All of the waveguide modes shown in the

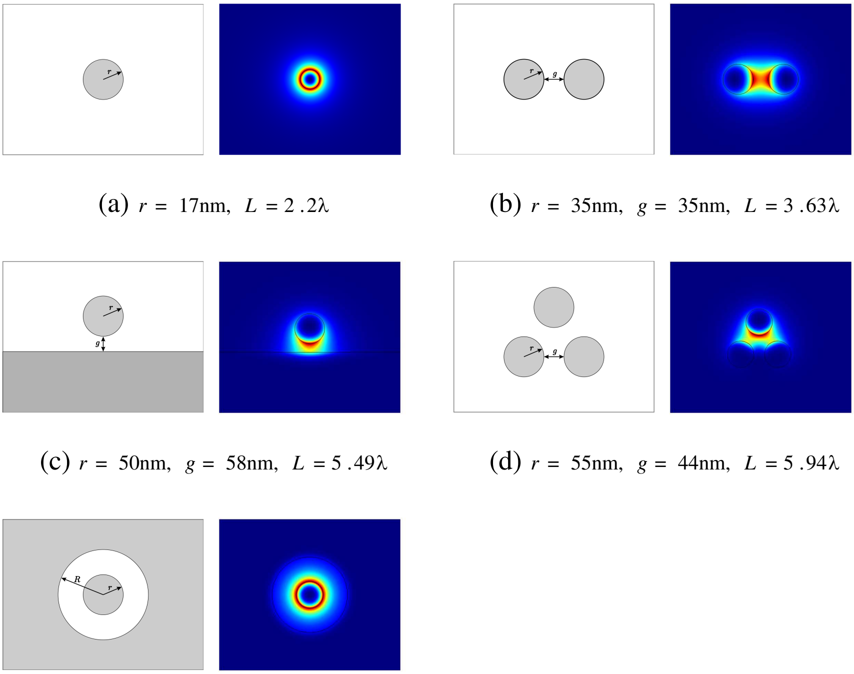

(a) $r = 17\text{nm}$, $L = 2.2\lambda$

(b) $r = 35\text{nm}$, $g = 35\text{nm}$, $L = 3.63\lambda$

(c) $r = 50\text{nm}$, $g = 58\text{nm}$, $L = 5.49\lambda$

(d) $r = 55\text{nm}$, $g = 44\text{nm}$, $L = 5.94\lambda$

(e) $r = 55\text{nm}$, $R = 155\text{nm}$, $L = 7.12\lambda$

Figure 2. Schematics and magnetic energy distributions of several simple plasmonic waveguide modes. The shaded areas are assumed to be gold and the unshaded ones represent vacuum. Dimensions and the propagation lengths of modes are listed under the drawings.

Fig. 2 are designed to have $\sigma_{\mathbf{H}} = 100\,\text{nm}$. The propagation lengths of the modes and waveguide dimensions are also presented in the Fig. 2. As expected all of the propagation lengths are smaller than the theoretical upper limit. Coaxial waveguide (Fig. 2(e)) has the longest propagation length among these waveguides. However, it is almost a factor of 9 smaller than the upper bound. More sophisticated waveguides and waveguides with graded index materials (with the same material loss merit factors) are expected to have longer propagation length and better achieve the upper bound.

6. CONCLUSION

In summary, it was shown that there is a fundamental trade-off between loss and confinement of a general electromagnetic waveguide. As the confinement increases, the material loss due to waveguide material also increases which decreases the propagation length of the waveguide mode.

ACKNOWLEDGMENT

We wish to acknowledge supports from the National Science and Engineering Council (NSERC) of Canada and Research In Motion (RIM).

REFERENCES

1. Ozbay, E., "Plasmonics: Merging photonics and electronics at nanoscale dimensions," *Science*, Vol. 311, No. 5758, 189–193, 2006.
2. Barnes, W. L., A. Dereux, and T. W. Ebbesen, "Surface plasmon subwavelength optics," *Nature*, Vol. 424, No. 6950, 824–830, London, 2003.
3. Bozhevolnyi, S. I., V. S. Volkov, E. Devaux, J.-Y. Laluet, and T. W. Ebbesen, "Channel plasmon subwavelength waveguide components including interferometers and ring resonators," *Nature*, Vol. 440, No. 7083, 508–511, London, 2006.
4. Zia, R., M. D. Selker, P. B. Catrysse, and M. L. Brongersma, "Geometries and materials for subwavelength surface plasmon modes," *J. Opt. Soc. Am. A*, Vol. 21, No. 12, 2442–2446, 2004.
5. Dionne, J. A., L. A. Sweatlock, H. A. Atwater, and A. Polman, "Plasmon slot waveguides: Towards chip-scale propagation with subwavelength-scale localization," *Phys. Rev. B*, Vol. 73, No. 3, 035407, 2006.
6. Baida F. I., A. Belkhir, D. V. Labeke, and O. Lamrous, "Subwavelength metallic coaxial waveguides in the optical range: Role of the plasmonic modes," *Phys. Rev. B*, Vol. 74, No. 20, 205419, 2006.
7. Gramotnev, D. K. and D. F. P. Pile, "Single-mode subwavelength waveguide with channel plasmon-polaritons in triangular grooves on a metal surface," *App. Phys. Lett.* , Vol. 85, No. 26, 6323–6325, 2004.

8. Oulton, R. F., V. J. Sorger, D. A. Genov, D. F. P. Pile, and X. Zhang, "A hybrid plasmonic waveguide for subwavelength confinement and long-range propagation," *Nat. Photon.*, Vol. 2, No. 8, 496–500, 2008.
9. Rybczynski, J., K. Kempa, A. Herczynski, Y. Wang, M. J. Naughton, and Z. F. Ren, "Subwavelength waveguide for visible light," *App. Phys. Lett.* , Vol. 90, No. 2, 21104, 2007.
10. Pile, D. F. P. and D. K. Gramotnev, "Plasmonic subwavelength waveguides: Next to zero losses at sharp bends," *Optics Lett.*, Vol. 30, No. 10, 1186–1188, 2005.
11. Oulton, R. F., V. J. Sorger, T. Zentgraf, R.-M. Ma, C. Gladden, L. Dai, G. Bartal, and X. Zhang, "Plasmon lasers at deep subwavelength scale," *Nature*, Vol. 461, No. 8364, 629–632, London, 2009.
12. Veronis, G. and S. Fan, "Bends and splitters in metal-dielectric-metal subwavelength plasmonic waveguides," *Appl. Phys. Lett.*, Vol. 85, No. 13, 131102, 2005.
13. Hosseini, A. and Y. Massoud, "Nanoscale surface plasmon based resonator using rectangular geometry," *Appl. Phys. Lett.*, Vol. 90, No. 18, 181102, 2007.
14. Boltasseva, A., T. Nikolajsen, K. Leosson, K. Kjaer, M. S. Larsen, and S. I. Bozhevolnyi, "Integrated optical components utilizing long-range surface plasmon polaritons," *J. Lightw. Technol.*, Vol. 1, No. 1, 413–422, 2005.
15. Pile, D. F. P., T. Ogawa, D. K. Gramotnev, and Y. Matsuzaki, "Two-dimensionally localized modes of a nanoscale gap plasmon waveguide," *App. Phys. Lett.*, Vol. 87, No. 26, 2005.
16. Chen, L., J. Shakya, and M. Lipson, "Subwavelength confinement in an integrated metal slot waveguide on silicon," *Optics Lett.*, Vol. 31, No. 14, 2133–2135, 2006.
17. Palik, E. D., *Handbook of Optical Constants of Solids*, Vol. I, Academic Press, 1998.